NEAR-WAKE VORTICITY DYNAMICS
IN BLUFF BODY FLOWS

Hugh M. Blackburn

Division of Building, Construction and Engineering

Commonwealth Scientific and Industrial Research Organisation (CSIRO)

Highett, Victoria

AUSTRALIA

Ron D. Henderson

Graduate Aeronautical Laboratories

California Institute of Technology

Pasadena, California

USA

ABSTRACT

In this paper we examine the generation and transport of vorticity in the near-wake of a circular cylinder, based on results from 2D Navier–Stokes simulations for $Re = 500$. Simulation results are examined for the cases of a fixed cylinder, and for a cylinder in forced cross-flow oscillation. Generation and transport of vorticity in the base region is observed to play a central role in the vortex formation process and in the lock-in mechanism.

INTRODUCTION

The study of coupling between the flow in the wake of a circular cylinder and cylinder motion has important applications in structural, offshore and thermal power engineering. A significant feature of the cylinder-wake interaction is that the point in the motion cycle at which vortices are formed and released is sensitive to the frequency of cylinder oscillation. Experimental flow visualizations, such as those of Ongoren & Rockwell (1988), demonstrate this sensitivity for flows where the frequency of cylinder cross flow oscillation (f_o) is close to the Strouhal frequency for the fixed cylinder (f_v); the timing of vortex formation switches phase by approximately 180° over a very narrow range of cylinder oscillation frequencies. This also results in dramatic changes in the phase of vortex-induced forces on the cylinder, and affects the sign of time-averaged mechanical power flow between the moving cylinder and the flow. Since the sign of power transfer determines whether cross-flow oscillations will tend to increase or decrease in amplitude, the mechanics of this phase shift are of central interest in the study of vortex-induced vibration.

Part of the problem in understanding this fluid-structure interaction stems from difficulties in visualizating and measuring the large-scale separated flow near a moving body. More fundamentally, the flows are complex and time-varying, and there are few theoretical results available to guide interpretation. As a first step in understanding the physical processes involved, we have taken a direct numerical simulation approach. We present and discuss plots of vorticity contours in the near wake for 2D simulations at $Re = 500$ for a fixed cylinder, and for a cylinder in forced cross-flow oscillation.

NUMERICAL METHOD

A spectral element spatial discretization was employed in conjunction with a second-order time-splitting scheme to solve the 2D incompressible Navier–Stokes equations in a reference frame attached to the cylinder. To allow cylinder motion, frame acceleration terms are added to the Navier–Stokes equations, and the boundary conditions adjusted appropriately. The method and previous applications are detailed in Blackburn & Karniadakis (1993) and Blackburn & Henderson (1995). The solver uses a primitive-variable formulation and vorticity is computed in post-processing.

The mesh employed here is the same as the refined mesh, M_2, used in Blackburn & Henderson (1995), where the solution convergence was demonstrated. The overall dimensions of the mesh are: cross-flow dimension $25\,D$; outflow length $50\,D$. We illustrate results in a small region near the cylinder.

RESULTS

Near-wake vorticity contour plots are presented for the fixed cylinder and for the cylinder in forced cross-flow oscillation at an amplitude $A/D = 0.5$. Additional results, which cover a wider range of amplitudes and frequency ratios, may be found in Blackburn & Henderson (1995); there, greater emphasis was given to the far-wake vorticity dynamics. The instantaneous streamlines have also been studied, but are not presented here, to keep the complexity of the diagrams to a minimum — many of the features of

the near-wake velocity field can be deduced from the vorticity contours.

Four key theoretical results can be used as aids to interpretation. First, continuity demands that separation and attachment points must occur in pairs for a 2D body. Second, in the frame of reference of the body, separation and attachment occur at points of zero surface vorticity (Lighthill 1963). Third, vorticity production can only occur at a solid boundary in an incompressible flow in response to wall-tangential components of pressure gradient and/or boundary acceleration (Morton 1984). Fourth, for flow past a body that has no angular acceleration, the integral around the body perimeter of the flux of "total vorticity" (vorticity integrated over domain area) is zero at every instant, due to the continuity of the pressure field:

$$\oint -\nu \frac{\partial \omega}{\partial n}\, dS = 0. \tag{1}$$

Fixed Cylinder

Vorticity contours for flow past a fixed cylinder at $Re = 500$ are shown in Fig. 1; the five frames show the half of the (periodic) vortex shedding cycle during which lift force acts in the upwards direction, starting and ending at times of zero lift. Attachment and separation points are labelled **A** and **S** respectively. The Strouhal frequency $St = f_v U/D = 0.227$.

There are three separation/reattachment pairs shown in Fig. 1a; the two pairs on the basal (rear) surface form the terminating points for two separation bubbles — regions of flow where the bounding streamline starts and ends on the surface of the body. These bubbles have greater areas than the two small black regions of counter-clockwise (CCW) vorticity on the basal surface. Associated with this streamline topology there is a downflow in the base region of the cylinder which advects vorticity of clockwise (CW) sign (grey contours), *produced on the basal surface of the cylinder*, towards the lower shear layer. The lower shear layer has at this stage completed the formation of a large region of CCW signed vorticity, which contains a detached region of circulating flow (closed streamline loops). This region is accelerating away from the cylinder.

In Fig. 1b the two speratation bubbles have coalesced into a single larger bubble, as indicated by the coalescence of the two regions of CCW vorticity on the basal surface. At this stage there are two separation/reattachment pairs. Since the region of CCW vorticity on the basal surface is growing with time, it can be inferred that CCW vorticity is being produced on the basal surface in Figs. 1a and 1b by a pressure gradient, where the pressure is decreasing bottom to top. At the same time, this vorticity begins to be advected towards the upper shear layer by flow in the recirculation bubble. Since the bubble is still closed at the instant of Fig. 1c, there can be no direct advective transport of CCW vorticity to the upper shear layer, although diffusive transport (normal to the contour lines) will produce significant cross-annihilation.

In Fig. 1d, a very small region of CW vorticity appears on the upper basal surface, enveloped by CCW vorticity. This signals the return to three separa-

Figure 1: FIXED CYLINDER, $Re = 500$. VORTICITY CONTOURS FOR THE HALF OF THE VORTEX SHEDDING CYCLE DURING WHICH LIFT IS POSITIVE.

tion/reattachment pairs, and formation of a small separation bubble on the upper basal surface. Significantly, this event implies the closure of large separation bubble with CW circulation that evolved in Figs. 1a and 1b; this bubble now forms a closed streamline loop and the CCW shear layer formed in the base region can now advect directly towards the upper shear layer.
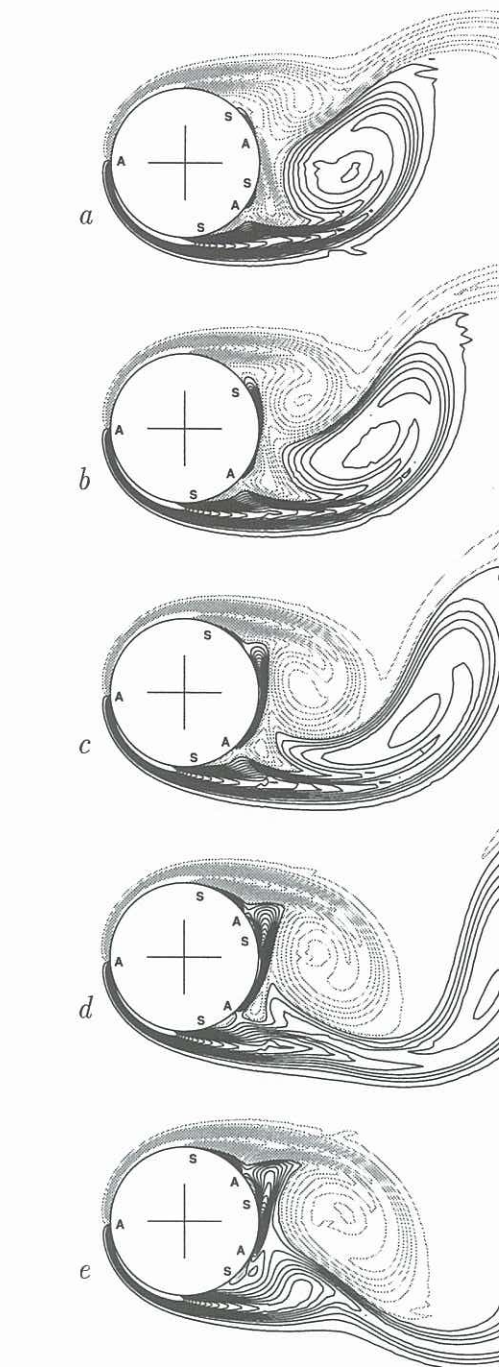
In summary, a very significant feature of Fig. 1 is the formation and advection of a comparatively strong shear layer in the base region. The sign of vorticity in this basal shear layer always opposes the sign of the main shear layer towards which it advects.
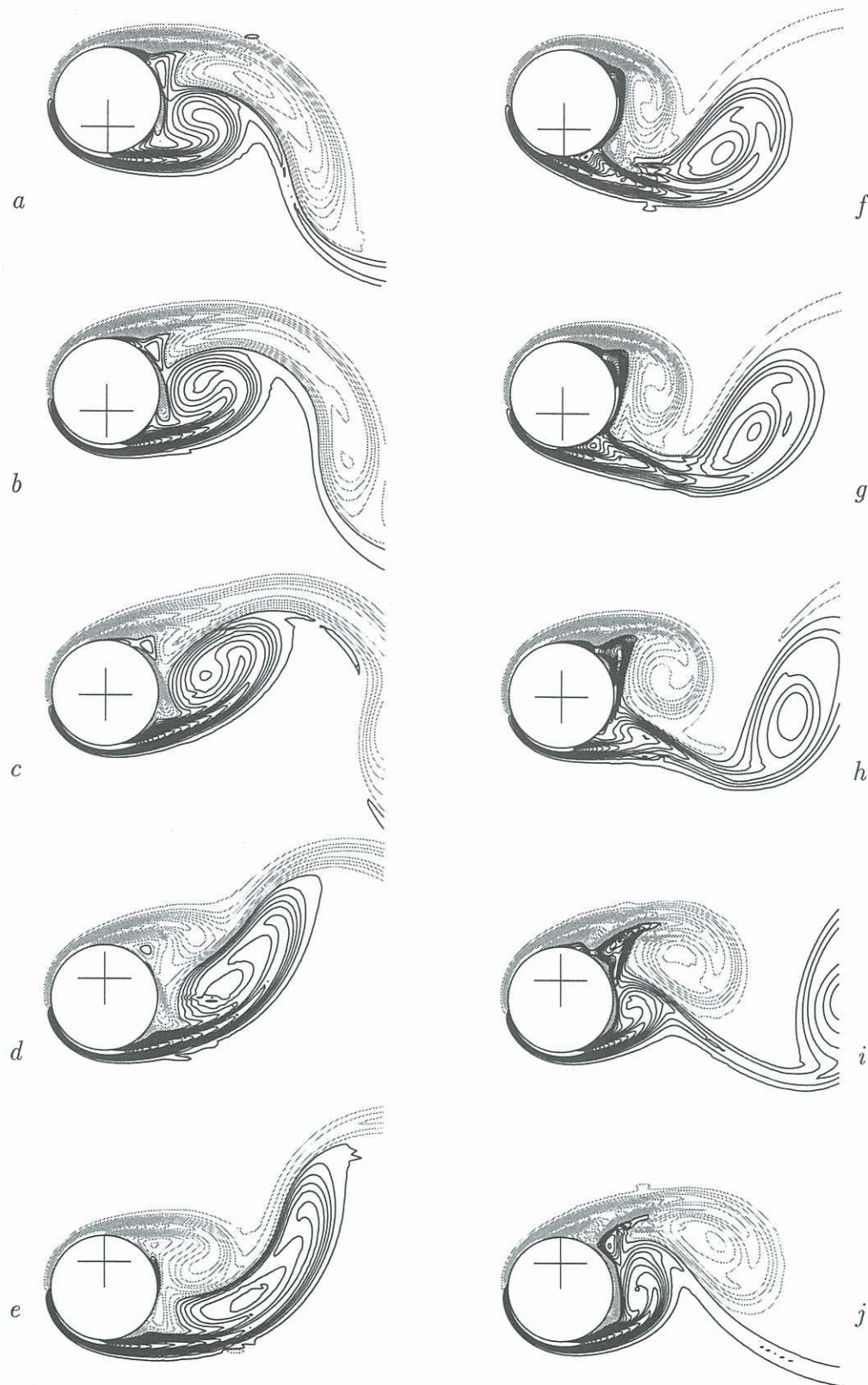
Figure 2: HALF A MOTION CYCLE FOR AN OSCILLATING CYLINDER, AMPLITUDE $A/D = 0.5$. $A-E$: $F_O/F_V = 0.89$, POWER TRANSFER TO BODY. $F-J$: $F_O/F_V = 0.95$, POWER TRANSFER TO FLUID.

This feature of the very near-wake has attracted little previous comment, presumably as a consequence of observational difficulties in physical experiments: as a result of the intricate folding of material lines in the base region (Perry, Chong & Lim 1982) it becomes very difficult to make conclusions about vorticity transport based on studies of marker (dye) transport. For example, one of the few models for the

bluff-body vortex shedding process (Gerrard 1966) describes vortex formation solely in terms of the interaction between the shear layers formed on the upper and lower front surface of the cylinder. According to the results presented in Fig. 1, Gerrard's model is incomplete.

Oscillating Cylinder

Examples of vorticity contours for cylinders in forced cross-flow oscillation are shown in Fig. 2. The two sets of results (a–e and f–j) shown are for an amplitude of oscillation $A/D = 0.5$. Each set shows a half cycle of cylinder motion, starting with the cylinder in its uppermost position. In both cases the frequency of vortex shedding was the same as that of the body motion. The difference between the two sets resulted from employing different driving frequencies: for Fig. 2a–e, $f_o/f_v = 0.89$, while for Fig. 2f–j, $f_o/f_v = 0.95$. Although the computations were performed in a frame of reference attached to the cylinder, they are visualized here in a fixed reference frame (indicated by the cross-hairs). This has significant effect on the instantaneous streamlines, but none on the contours of vorticity.

There is obviously a marked difference in phase of vortex formation and shedding between the two sets of results. As noted in the introduction, sensitivity to driving frequency is a well-known feature of this fluid-structure interaction. The change of phase of shedding is reflected in the flow of mechanical power between the cylinder and the fluid flow (the total energy transferred per cycle is the time integral of the product of lift force and cylinder velocity). In the case of Fig. 2a–e the mechanical energy transferred to the body per motion cycle is positive, while for Fig. 2f–j it is negative: this corresponds to negative and positive "aerodynamic damping" respectively. In addition, the magnitudes of peak lift coefficients fall respectively below and above that for the fixed cylinder.

Compared to the fixed cylinder, where the only mechanism for vorticity production is the tangential pressure gradient on the cylinder surface, an additional mechanism comes into play for the oscillating cylinder: the surface-tangential component of cylinder acceleration, which has maximum effect on the front and rear surfaces but none at the upper and lower points of the cylinder. When the cylinder accelerates downwards (as in frames a–c and f–h) this mechanism acts to produce fluxes of CW vorticity on the front cylinder face and CCW vorticity on the rear face. Quantitatively these fluxes are of larger magnitude in f–j since the acceleration is larger than in a–e by the square of the ratios of the frequency ratios (a factor of 1.14).

Again the formation of basal shear layers and their interaction with the main shear layers is obviously significant. In both Fig. 2a and f a region of CCW vorticity near the base of the cylinder is being advected towards the upper CW shear layer. In Fig. 2f, however, the interaction is much stronger for a number of reasons. First, the diffusive cross-annihilation must be far stronger, since the contour lines are more

closely-spaced. Second, the CCW basal shear layer is growing in strength at the same time as it is advected towards the upper main shear layer, in direct contrast to the case in Fig. 2a, where CCW vorticity is being annihilated in the upper base region.

Now we are in a position to propose a lock-in mechanism. The key feature is the relative strengths of the pressure gradient and tangential acceleration vorticity production mechanisms on the basal surface. In the case of an oscillating body, shear layers would tend to roll up first on the side of the wake towards which the body is moving, as in Fig. 2a–e. Pressure gradients associated with this rollup tend to induce vorticity of opposite sign on the basal surface (as in a and b). The surface-acceleration vortcity generation mechanism opposes this production, but is not strong enough to override it. At the higher oscillation frequency in Fig. 2f–j, the tangential-acceleration production mechanism has been able to override the pressure-gradient mechanism. A very intense basal shear layer forms, inducing earlier rollup of the main shear layer from the opposite side of the cylinder than occurs in the lower frequency case — in turn there is a feed-back effect whereby the pressure gradient produced by the rollup of the main shear layer reinforces the tangential acceleration mechanism. The strength of the shear layer that is rolling up is enhanced, as indicated by the integral constraint, eq. (1).

CONCLUSIONS

Production and advection of basal shear layers has a significant effect on the vortex formation process. For flows past oscillating bodies, it is suggested that the strength and timing of basal vorticity production is central to the mechanism of lock-in.

REFERENCES

Blackburn, H. & Henderson, R. (1995). Wake dynamics in flow past an oscillating cylinder, *9th Int. Conf. Num. Meth. Laminar & Turb. Flow*, Atlanta.

Blackburn, H. M. & Karniadakis, G. E. (1993). Two- and three-dimensional simulations of vortex-induced vibration of a circular cylinder, *3rd Intnl Offshore & Polar Engng Conf.*, Vol. III, Singapore, pp. 715–720.

Gerrard, J. H. (1966). The mechanics of the formation region of vortices behind bluff bodies, *J. Fluid Mech.* **25**(2): 401–413.

Lighthill, M. J. (1963). II. Boundary Layer Theory, *in* L. Rosenhead (ed.), *Laminar Boundary Layers*, Oxford University Press, pp. 46–103.

Morton, B. R. (1984). The generation and decay of vorticity, *Geophys. Astrophys. Fluid Dyn.* **28**: 277–308.

Ongoren, A. & Rockwell, D. (1988). Flow structure from an oscillating cylinder. Part 1., *J. Fluid Mech.* **191**: 197–223.

Perry, A. E., Chong, M. S. & Lim, T. T. (1982). The vortex-shedding process behind two-dimensional bluff bodies, *J. Fluid Mech.* **116**: 77–90.